online data

Human CHMP6, a myristoylated ESCRT-III protein, interacts directly with an ESCRT-II component EAP20 and regulates endosomal cargo sorting

Chiharu YORIKAWA*, Hideki SHIBATA*, Satoshi WAGURI†, Kazumi HATTA*, Mio HORII*, Keiichi KATOH*, Toshihide KOBAYASHI‡, Yasuo UCHIYAMA† and Masatoshi MAKI*[1]

*Department of Applied Molecular Biosciences, Graduate School of Bioagricultural Sciences, Nagoya University, Furo-cho, Chikusa-ku, Nagoya 464-8601, Japan, †Department of Cell Biology and Neuroscience A1, Osaka University Graduate School of Medicine, Yamadaoka 2-2, Suita, Osaka 565-0871, Japan, and ‡Supra-Biomolecular System Research Group, RIKEN, 2-1 Hirosawa, Wako-shi, Saitama 351-0198, Japan

CHMP6 (charged multivesicular body protein 6) is a human orthologue of yeast Vps (vacuolar protein sorting) 20, a component of ESCRT (endosomal sorting complex required for transport)-III. Various CHMP6 orthologues in organisms ranging from yeast to humans contain the N-myristoylation consensus sequence at each N-terminus. Metabolic labelling of HEK-293 (human embryonic kidney) cells showed the incorporation of [^{3}H]myristate into CHMP6 fused C-terminally to GFP (green fluorescent protein) (CHMP6–GFP). Interactions of CHMP6 with another ESCRT-III component CHMP4b/Shax [Snf7 (sucrose non-fermenting 7) homologue associated with Alix] 1, one of three paralogues of human Vps32/Snf7, and with EAP20 (ELL-associated protein 20), a human counterpart of yeast Vps25 and component of ESCRT-II, were observed by co-immunoprecipitation of epitope-tagged proteins expressed in HEK-293 cells. The *in vitro* pull-down assays using their recombinant proteins purified from *Escherichia coli* demonstrated direct physical interactions which were mediated by the N-terminal basic half of CHMP6. Overexpressed CHMP6-GFP in HeLa cells exhibited a punctate distribution throughout the cytoplasm especially in the perinuclear area, as revealed by fluorescence microscopic analysis. Accumulation of LBPA (lysobisphosphatidic acid), a major phospholipid in internal vesicles of an MVB (multivesicular body), was observed in the CHMP6–GFP-localizing area. FLAG-tagged EAP20 distributed diffusely, but exhibited a punctate distribution on co-expression with CHMP6–GFP. Overexpression of CHMP6–GFP caused reduction of transferrin receptors on the plasma membrane surface, but caused their accumulation in the cytoplasm. Ubiquitinated proteins and endocytosed EGF continuously accumulated in CHMP6–GFP-expressing cells. These results suggest that CHMP6 acts as an acceptor for ESCRT-II on endosomal membranes and regulates cargo sorting.

Key words: charged multivesicular body protein family (CHMP family), EAP20, endosomal sorting complex required for transport (ESCRT), lysobisphosphatidic acid (LBPA), multivesicular endosome, N-myristoylation.

INTRODUCTION

Endosomes are intracellular membrane-bounded compartments that have critical roles in co-ordinating vesicular transport between the TGN (*trans*-Golgi network), the plasma membrane and lysosomes (see [1] for a review and references therein). There are different types of endosomal compartments distinguishable by pH, morphology, and compositions of proteins and lipids [2,3]. While early endosomes tend to be tubular and are located towards the cell periphery, late endosomes are more spherical and are often oriented closer to the nucleus. An MVB (multivesicular body) is defined as an endosome that contains a characteristic accumulation of vesicles in its lumen, as shown by morphological observation, and such bodies are often seen in late endosomes [4].

Binding to ligands induces clustering of cell-surface growth factor receptors in clathrin-coated regions of the plasma membrane, which bud into the cytosol to form vesicles that are subsequently delivered to endosomal compartments. The destination of the internalized receptor depends on sorting at the stage of early endosomes. EGF (epidermal growth factor) receptors are transported via the MVB lumen to lysosomes for degradation. In these processes, ubiquitination of receptors and of associated proteins serves as a signal for sorting of the tagged cargo into the luminal vesicles of MVB [5,6]. On the other hand, recycling receptors such as TfR (transferrin receptor) and LDLR (low-density lipoprotein receptor) are devoid of ubiquitin signals. They are transported to the tubular extensions of early endosomes and recycling endosomes, from where they are routed back to the plasma membrane.

Recently, a group of yeast Vps (vacuolar protein sorting) proteins have been identified by genetic analyses as factors required for MVB formation, and the functional loss of any individual class E Vps protein results in formation of a so-called class E compartment, which is characterized by an aberrantly enlarged pre-vacuolar endosome-like organelle [7]. Most class E Vps proteins, which exist predominantly as soluble proteins or subcomplexes, are sequentially recruited from the cytosol to

Abbreviations used: AIP1, apoptosis-linked-gene-2-interacting protein 1; ALG-2, apoptosis-linked gene 2; Alix, ALG-2-interacting protein X; CBB, Coomassie Brilliant Blue R-250; CHMP, charged multivesicular body protein; CHMP6CT, C-terminal half of CHMP6; CHMP6NT, N-terminal half of CHMP6; DMEM, Dulbecco's modified Eagle's medium; EAP20, ELL-associated protein 20; EEA1, early endosome antigen 1; EGF, epidermal growth factor; EGFP, enhanced green fluorescent protein; ESCRT, endosomal sorting complex required for transport; FBS, foetal bovine serum; GFP, green fluorescent protein; GST, glutathione S-transferase; IPTG, isopropyl β-D-thiogalactoside; Lamp-1, lysosome-associated membrane protein 1; LBPA, lysobisphosphatidic acid; mAb, monoclonal antibody; MBP, maltose-binding protein; MVB, multivesicular body; MVL, multivesicular liposome; Rh–EGF, tetramethylrhodamine–EGF; Rh–Tf, tetramethylrhodamine–transferrin; Shax, Snf7 (sucrose non-fermenting 7) homologue associated with Alix; SKD1, suppressor of potassium transport growth defect 1; Snf7, sucrose non-fermenting 7; TfR, transferrin receptor; TGN, *trans*-Golgi network; Trx, thioredoxin; Vps, vacuolar protein sorting; WT, wild-type.

[1] To whom correspondence should be addressed (email mmaki@agr.nagoya-u.ac.jp).

the sites of MVB formation and assemble a machinery termed ESCRT (endosomal sorting complex required for transport) [8–10]. At the endosome, ubiquitinated proteins are first recognized by Vps27, and are then transferred to recruited ESCRT-I (Vps23, Vps28 and Vps37) during MVB sorting [11,12]. ESCRT-I is then thought to activate functions of ESCRT-II (Vps22, Vps25 and Vps36) in the recruitment and oligomerization of small coiled-coil proteins (Vps2, Vps20, Vps24 and Vps32/Snf7) to form ESCRT-III. Mammalian orthologues of ESCRT components have been shown to be involved in the process of outward budding of virus particles from the plasma membrane [13–15]. Moreover, Alix [ALG-2 (apoptosis-linked gene 2)-interacting protein X]/AIP1 (ALG-2-interacting protein 1; a mammalian orthologue of yeast Class E Vps31/Bro1) interacts with viral Gag proteins and serves as a bridge between the selected components of ESCRT-I and ESCRT-III, i.e. Tsg101 and a mammalian orthologue of yeast Snf7 named CHMP (charged MVB protein) 4 respectively. From the viewpoint of membrane topology, this virus budding process is similar to invagination at the endosomal membrane during MVB sorting [16,17].

Human CHMP1 has been reported to be a protein that is involved in vesicle trafficking [18], and its homologues found in the human genome database are now collectively called the CHMP family. They are structurally similar to the yeast ESCRT-III components, and are thus candidates for the human counterparts playing still unclarified roles in invagination of endosomal membranes to form MVBs [16]. They are coiled-coil proteins of approx. 200 amino acid residues and exhibit an uneven distribution of charged residues, resulting in creation of basic and acidic regions in the N-terminal half and C-terminal half respectively. Although there have been extensive genetic and cell-biological studies on yeast ESCRT-III components, little is known about the biochemical properties and functions of the mammalian counterparts in the MVB sorting pathway. It remains to be established whether mammalian ESCRT-III components function by the same mechanism as that proposed for yeast Vps sorting at the MVB membrane, or by a similar, but distinct, mechanism that relies on different protein–protein interactions.

We previously identified three CHMP4 isoforms (CHMP4a, b and c; also named Shax2/CHMP4B/Snf7-2, Shax1/CHMP4A/Snf7-1 and Shax3/CHMP4C/Snf7-3 respectively) as novel Alix/AIP1-interacting proteins that are structurally similar to yeast Snf7, and we investigated the roles of CHMP4b in endosomal sorting [19]. Among the three CHMP4 isoforms, CHMP4b was found to be a major binding partner of Alix/AIP1, as judged by their mRNA expression levels and strength of interactions *in vitro* using their recombinant fusion proteins [20]. In the present study, to gain more insights into functions of ESCRT-III components in mammalian MVB sorting, we focused on CHMP6, assuming that it functions as a key component of ESCRT-III working at the later stage of MVB formation, because CHMP6 is a human orthologue of yeast Vps20, which was suggested to be N-myristoylated and is known to interact with Snf7 to form an ESCRT-III subcomplex [9]. We first demonstrated that CHMP6 is indeed N-myristoylated *in vivo*. The N-terminal half of CHMP6 interacts physically not only with CHMP4b, but also with EAP20 (ELL-associated protein 20), which is a human orthologue of yeast Vps25 that belongs to ESCRT-II [7]. We also found that exogenously overexpressed CHMP6–GFP (green fluorescent protein) fusion protein exhibits a punctate distribution in HeLa cells, causes accumulation of ubiquitinated proteins in endosomes and disturbs endosomal sorting of TfR and endocytosed EGF. These results suggest that the ESCRT-III component CHMP6 participates in MVB formation by acting as an acceptor for ESCRT-II on the endosomal membrane.

MATERIALS AND METHODS

cDNA cloning and plasmid construction

Human cDNAs for CHMP6 and EAP20 were cloned from a Human Fetus Marathon-Ready™ cDNA (Clontech) library by the PCR method with a proofreading thermostable *Pfu* DNA polymerase (Stratagene), using specific primers designed on the basis of the registered cDNA sequences (GenBank® accession numbers BC010108 and BC006282 respectively). In order to insert a flexible oligopeptide linker between CHMP6 and EGFP (enhanced green fluorescence protein), a pSGG-GFP vector was constructed by ligating a synthetic oligonucleotide block encoding an SGG sequence (three tandem repeats of Ser-Gly-Gly: plus strand, 5′-CGGATCCAAGCGGAGGCTCTGGCGGATCTGGCGGCCGC-3′; minus strand, 5′-GATCGCGGCCGCCAGATCCGCCAGAGCCTCCGCTTGGATCCGGTAC-3′) into the *Kpn*I/*Bam*HI site of pEGFP-N1 (Clontech). pCHMP6^{G2A}-GFP, which has a point mutation at amino acid 2 (a substitution of alanine for glycine), was obtained by PCR-based site-directed mutagenesis using a QuikChange site-directed mutagenesis kit (Stratagene) according to the manufacturer's instructions, and the mutation was confirmed by DNA sequencing.

Bacterial expression plasmids for preparation of recombinant CHMP6 proteins fused with GST (glutathione S-transferase) were constructed by conventional methods using restriction enzyme digestion, isolation of fragments, and ligation into a GST-fusion vector, pGEX-4T-1 (Amersham Biosciences). DNA fragments corresponding to EAP20 were ligated into the *Eco*RI site of either pMAL-c2 (New England Biolabs) for the expression of MBP (maltose-binding protein)-fused EAP20 or pCMV-3 × FLAG-A [19] for the expression of FLAG-tagged EAP20. The obtained constructs were designated pMBP-EAP20 and pFLAG-EAP20 respectively. Constructions of pFLAG-CHMP4b and pTrx-His-CHMP4b (where Trx is thioredoxin and His is His_6) have been described previously [19,20].

Antibodies

The following mouse mAbs (monoclonal antibodies) were purchased: anti-EEA1 (early endosome antigen 1) mAb (Transduction Laboratories), anti-Lamp-1 (lysosomal membrane protein-1)/CD107a mAb (Pharmingen), anti-multiubiquitin mAb (FK2) (MBL, Nagoya, Japan), anti-FLAG mAb (M2) (Stratagene) and anti-GFP mAb (B2) (Santa Cruz Biotechnology). Preparation of a mouse mAb against LBPA (lysobisphosphatidic acid) has been described previously [2]. Anti-TfR mAb was kindly provided by Dr T. Yoshimori (National Institute of Genetics, Mishima, Japan). Rabbit anti-GFP antiserum and Cy3-labelled goat anti-mouse IgG used for indirect immunofluorescence analyses were purchased from Molecular Probes and Amersham Biosciences respectively. Horseradish-peroxidase-conjugated goat anti-mouse and anti-rabbit IgGs were obtained from Jackson Immunoresearch Laboratories.

Cell culture and DNA transfection

HEK-293 (human embryonic kidney) and HeLa cells were cultured in DMEM (Dulbecco's modified Eagle's medium) supplemented with 10 % heat-inactivated FBS (foetal bovine serum), 100 units/ml penicillin and 100 μg/ml streptomycin at 37 °C under humidified air containing 5 % CO_2. At 1 day after HEK-293 cells or HeLa cells had been seeded, the cells were transfected with the expression plasmid DNAs by the conventional calcium phosphate precipitation method for HEK-293 cells and by using FuGENE 6 (Roche Applied Science) for HeLa cells. After 24 h, cells were harvested and analysed.

[^{3}H]myristic acid uptake assay

At 1 day after HEK-293 cells (1.5×10^5) were transfected with each expression plasmid DNA of GFP-fusion protein, the cells were biosynthetically labelled for 16 h with [^{3}H]myristic acid (0.2 mCi/ml) (Amersham Biosciences) in DMEM supplemented with 5 % heat-inactivated FBS. Labelled cells were washed with PBS and lysed in lysis buffer A (10 mM Hepes/NaOH, pH 7.4, 150 mM NaCl, 1 % Nonidet P40, 2 mM EDTA, 2 mM EGTA, 0.1 mM Pefabloc, 25 μg/ml leupeptin, 1 μM E-64 and 1 μM pepstatin). GFP-fusion proteins in supernatants obtained by centrifugation at 10000 ***g*** for 10 min were immunoprecipitated with anti-GFP antiserum and Protein G–Sepharose 4 Fast Flow (Amersham Biosciences). Immunoprecipitated proteins were resolved by SDS/PAGE. The gel was treated with Amplify™ Fluorographic Reagent (Amersham Biosciences), as directed by the manufacturer, and exposed for 12 days to Hyperfilm MP (Amersham Biosciences) at − 80 °C using an intensifying screen.

Expression and purification of recombinant proteins

Escherichia coli BL21 cells were transformed with each constructed GST-fusion protein expression plasmid (pGEX4T-1, pGST-CHMP6, pGST-CHMP6NT or pGST-CHMP6CT, where CHMP6NT and CHMPCT are the N- and C-terminal halves of CHMP6 respectively). GST-fusion protein expression was induced with 0.5 mM IPTG (isopropyl β-D-thiogalactoside) for 3 h at 23 °C, and the proteins were purified by binding to glutathione–Sepharose 4B (Amersham Biosciences) according to the manufacturer's instructions. MBP-fusion proteins were similarly expressed in *E. coli* BL21 cells, except that IPTG induction was performed for 3 h at 37 °C, and the recombinant proteins were purified by binding to amylose resin (New England Biolabs) according to the manufacturer's instructions. Trx–His–CHMP4b was purified as described previously [20].

Co-immunoprecipitation assay

At 1 day after HEK-293 cells (3×10^6) had been seeded, they were transfected with 3 μg of the expression plasmid DNAs. After 24 h, cells were harvested with PBS and lysed in lysis buffer B (10 mM Hepes/NaOH, pH 7.4, 0.2 % Nonidet P40, 142.5 mM KCl, 0.1 mM Pefabloc, 25 μg/ml leupeptin, 1 μM E-64 and 1 μM pepstatin). Supernatants obtained by centrifugation at 10000 ***g*** were incubated with an appropriate antibody at 4 °C for 1 h, and then Protein G–Sepharose was added and the mixture was incubated for a further 1 h. The Sepharose beads were then washed with lysis buffer B three times and subjected to Western blot analysis using an appropriate antibody. Immunoreactive bands were visualized by the chemiluminescent method using Super Signal West Pico Chemiluminescent Substrate (Pierce).

Immunofluorescence microscopic analysis

At 1 day after HeLa cells (1×10^4) had been seeded on to 18 mm^2 coverslips in 3-cm-diameter dishes, they were transfected with 1 μg of the respective expression plasmid DNA. After 24 h, cells were fixed in 4 % (w/v) paraformaldehyde in PBS and permeabilized in 0.1 % (v/v) Triton X-100 in PBS. After blocking with 0.1 % (w/v) gelatin in PBS at 37 °C for 30 min, the cells were processed for immunocytochemistry as described previously [21]. For LBPA immunostaining, the monoclonal antibody 6C4 [2] was incubated in the presence of 0.05 % (v/v) saponin without prior permeabilization. The fluorescence signals of GFP and Cy3-labelled goat anti-mouse IgG were analysed with a confocal laser-scanning microscope, LSM5 PASCAL (Zeiss, Göttingen, Germany).

Pull-down assay

In the case of the GST pull-down assay, a fixed amount of either Trx–His-fusion protein or MBP-fusion protein was mixed with GST-fusion protein in 200 μl of binding buffer (10 mM Tris/HCl, pH 7.5, 1 mM EDTA and 500 mM NaCl) containing 1 % (v/v) Triton X-100, and was shaken gently by rotation at 4 °C overnight. Glutathione–Sepharose 4B beads were then added, and incubation was continued for 30 min at 4 °C. In the case of the MBP pull-down assay, a fixed amount of GST-fusion protein was mixed gently with amylose-resin-bound MBP-fusion protein in 200 μl of binding buffer containing 0.1 % (v/v) Triton X-100 as described above. After extensive washing with the respective binding buffer, proteins were eluted with SDS/PAGE sample buffer and subjected to SDS/PAGE, and gels were then stained with CBB (Coomassie Brilliant Blue R-250).

Assays for binding and uptake of cell-surface receptor ligands

Assays for EGF uptake and transferrin binding to cell-surface receptors were performed essentially as described in [22], but with modifications as follows. At 1 day after transfection and culture on coverslips in 3-cm-diameter dishes, HeLa cells were incubated with serum-free medium (DMEM containing 10 mM Hepes/NaOH, pH 7.4, and 0.5 mg/ml BSA) for 1 h at 37 °C and then for 30 min at 4 °C. For the EGF uptake assay, a small volume (50 μl) of 0.5 μg/ml Rh–EGF (tetramethylrhodamine–EGF) (Molecular Probes) solution in the serum-free medium was poured on to coverslips, and cells were incubated for 1 h at 4 °C to allow binding of Rh–EGF to cell-surface receptors. The cells were then washed with the serum-free medium, and Rh–EGF uptake was initiated by incubating in DMEM containing 10 % (v/v) FBS for either 30 min or 5 h at 37 °C. Cells were washed with PBS, fixed in 4 % (w/v) paraformaldehyde in PBS, and then observed under a confocal laser-scanning microscope as described above. For the transferrin-binding assay, transfected HeLa cells on coverslips were pre-treated with the serum-free medium as described above and incubated with 50 μg/ml Rh–Tf (tetramethylrhodamine–transferrin) (Molecular Probes) in Hanks solution for 30 min at 4 °C. Cells were then washed, fixed, and observed under a confocal laser-scanning microscope.

RESULTS

Myristoylation of human CHMP6

A human cDNA encoding CHMP6 was cloned by PCR using a human foetus cDNA library as a template. The determined nucleotide sequence agrees with the registered sequence in the DNA data bank (GenBank® accession number BC010108, designated FLJ11749). Full-length or fragments of the obtained cDNAs were subcloned into various vectors for mammalian or *E. coli* expression either directly or after site-directed mutagenesis. Figure 1 shows schematic structures of various constructs used in the present study.

Human CHMP6 consists of 201 amino acid residues, and has two predicted coiled-coil structures (residues 10–94 and 119–145), each in the N-terminal half and the C-terminal half respectively. Basic and acid residues are clustered in the N-terminal region (residues 1–68; calculated pI = 12.08) and C-terminal region (residues 69–201; calculated pI = 3.93) respectively. CHMP6 proteins are highly conserved from yeast to mammals (30 % amino acid identity between the yeast and human sequences). Among yeast ESCRT-III components (Vps2, Vps20, Vps24 and Snf7/Vps32), only Vps20 is reported to have an N-myristoylation site [9]. Although the N-terminal sequence of human CHMP6 is

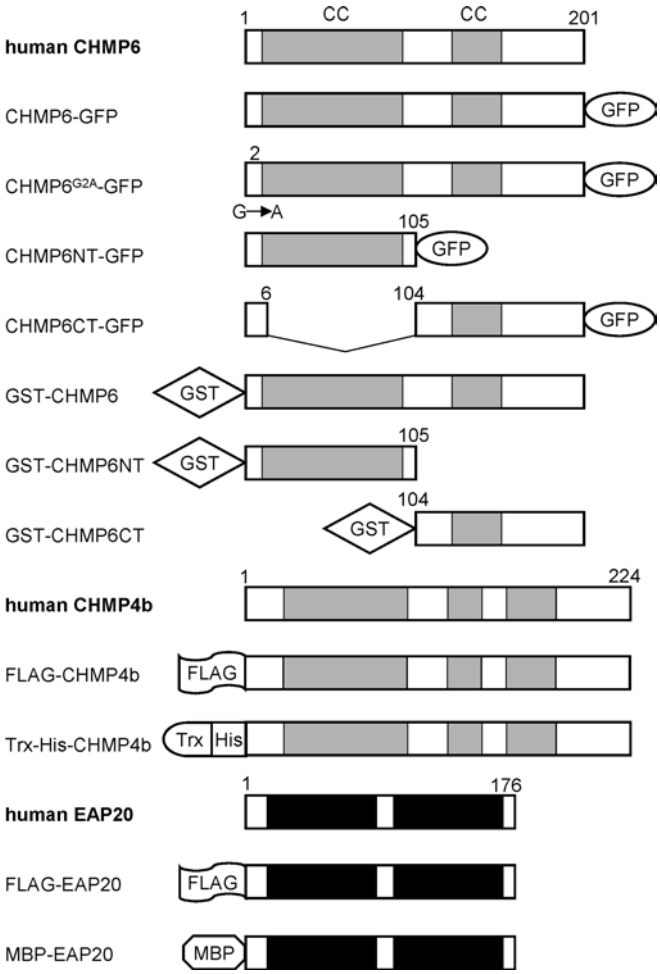

Figure 1 Schematic representation of various expression constructs used in the present study

Full-length deletion or point mutation constructs of CHMP6, CHMP4b or EAP20 were prepared as fusion proteins of GFP, FLAG, GST, Trx–His and MBP. The numbers denote the amino acid positions in each construct. The coiled-coil regions (CC) are indicated by grey boxes. CHMP6^{G2A}–GFP is the point mutant of critical residue 2 (substitution of alanine for glycine). Regions similar to WH (winged helix) domains of the yeast ESCRT-II components, whose structures were elucidated by X-ray crystalography [37,38], are indicated by closed boxes for EAP20.

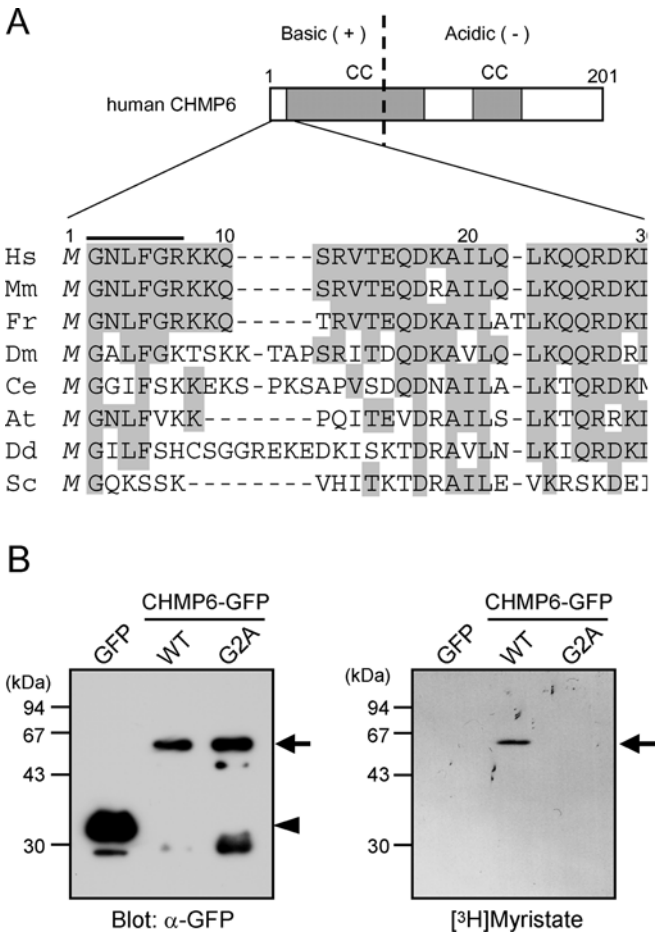

Figure 2 N-myristoylation of human CHMP6

(**A**) N-terminal amino acid sequences of human CHMP6 and its orthologues. A schematic representation of human CHMP6 is shown at the top. The vertical broken line divides the protein into two highly charged regions rich in basic and acidic residues respectively. Two coiled-coil regions (CC) predicted by using a program on the Internet (http://www.ch.embnet.org/software/COILS_form.html; window 21; values greater than 0.5) are indicated by grey boxes. The amino acid sequences were aligned using the default setting of ClustalX 1.83, a multiple sequence alignment program (http://www-igbmc.u-strasbg.fr/BioInfo/ClustalX/Top.html). A bar above the human sequence indicates a segment that matches an N-myristoylation pattern (PROSITE code PDOC00008) consisting of six residues where glycine is N-myristoylated. Organism names are abbreviated and sequences were taken either from GenBank® (accession numbers indicated in parentheses) or from each genome project home page for respective organisms (accession numbers indicated in brackets) as follows: Hs, *Homo sapiens* (BC010108); Mm, *Mus musculus* (XP_126613); Fr, *Fugu rubripes* [SINFRUP00000076922]; Dm, *Drosophila melanogaster* (NP_726213.1); Ce, *Caenorhabditis elegans* (NP_490762.1); At, *Arabidopsis thaliana* (AAM62458.1); Dd, *Dictyostelium discoideum* [DDB0187234]; Sc, *Saccharomyces cerevisiae* (NP_013794). (**B**) Metabolic labelling of CHMP6 with [^{3}H]myristic acid. HEK-293 cells transfected with pGFP, pGFP-CHMP6 or pGFP-CHMP6^{G2A} were cultured for 16 h with [^{3}H]myristic acid. GFP-fusion proteins were immunoprecipitated with GFP antiserum and analysed by SDS/PAGE, followed by immunoblotting with anti-GFP mAb (left-hand panel, unlabelled) or fluorography (right-hand panel, [^{3}H]myristate-labelled). Similar results were obtained in two independent experiments, and a representative Figure is shown. Arrows indicate CHMP6–GFP and CHMP6^{G2A}–GFP, and an arrowhead indicates GFP. Molecular mass sizes are indicated in kDa.

not conserved with that of yeast Vps20 (Figure 2A), it also possesses a putative N-myristoylation site. Moreover, the first six amino acid residues starting with glycine in each CHMP6 sequence from other organisms, except for *Arabidopsis*, are consistent with the consensus pattern of the N-myristoylation site, where the first glycine is N-myristoylated (PROSITE code PDOC00008, G-{EDRKHPFYW}-X_2-[STAGCN]-{P}, where braces indicate residues not allowed, X_2 is any two amino acids and square brackets indicate any one of the indicated residues). To determine whether the putative N-myristoylation site of human CHMP6 is indeed N-myristoylated *in vivo*, we performed metabolic labelling of HEK-293 cells using [^{3}H]myristic acid after cells had been transfected with pGFP, pCHMP6-GFP or pCHMP6^{G2A}-GFP (a putative N-myristoylation-defective mutant that has a substitution of alanine for the critical glycine). GFP-fusion proteins were immunoprecipitated with anti-GFP antibody, resolved by SDS/PAGE, and subjected to fluorography (Figure 2B). The radioactive signals were detected for the WT (wild-type) form of CHMP6–GFP, but not for the mutant form (CHMP6^{G2A}–GFP) or GFP (Figure 2B, right-hand panel), suggesting the addition of myristic acid to Gly^2, which becomes an N-terminal residue after translation initiation.

CHMP4b and EAP20 bind the N-terminal half of CHMP6

Babst et al. [10] suggested that there are genetic and physical interactions between ESCRT-II and ESCRT-III through Vps20

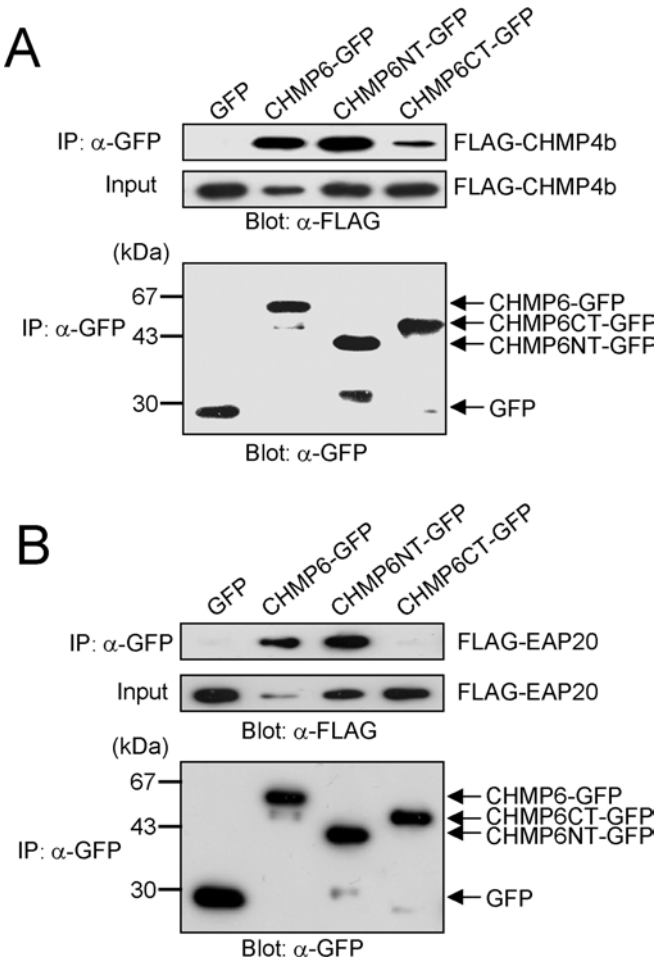

Figure 3 Dissection of CHMP6 interaction with CHMP4b and EAP20

(**A**) HEK-293 cells were co-transfected with pFLAG-CHMP4b and pGFP, pCHMP6-GFP, pCHMP6NT-GFP or pCHMP6CT-GFP. After 24 h, cells were lysed, and the 10000 ***g*** supernatants (Input) were immunoprecipitated (IP) with GFP antiserum. The supernatants and immunoprecipitates were analysed by Western blotting with anti-FLAG (two upper panels) and anti-GFP (α-GFP; lower panel) mAbs. (**B**) HEK-293 cells were co-transfected with pFLAG-EAP20 and pGFP, pCHMP6-GFP, pCHMP6NT-GFP or pCHMP6CT-GFP, and processed for immunoprecipitation followed by Western blotting as described in (**A**). Molecular mass sizes are indicated in kDa.

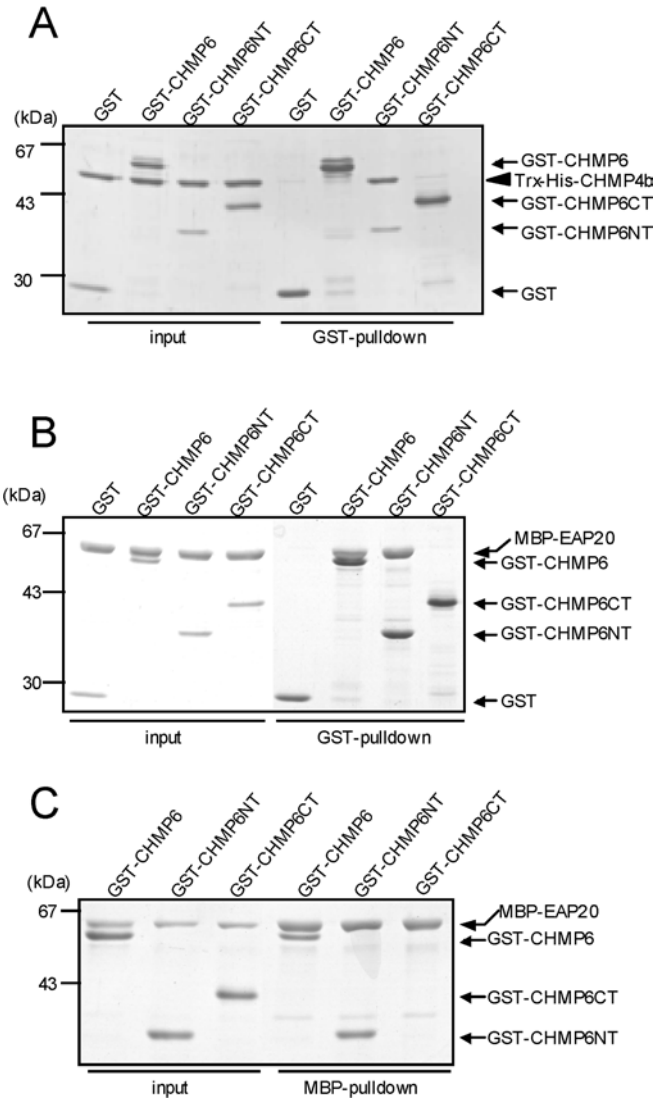

Figure 4 Direct interaction of CHMP6 with CHMP4b and EAP20

(**A**) CHMP4b-binding assay by GST pull-down. Recombinant protein of Trx–His–CHMP4b (400 pmol) was incubated with 200 pmol of GST or one of the GST-fusion proteins (full-length CHMP6 or truncated mutants) in 200 μl of binding buffer as described in the Materials and methods section, and glutathione–Sepharose beads were added. After the beads had been pelleted by centrifugation and washed, pulled-down proteins were analysed by SDS/PAGE and visualized by CBB staining. (**B**) EAP20-binding assay by GST pull-down. Recombinant protein of MBP–EAP20 (480 pmol) was incubated with GST (480 pmol) or one of the GST–CHMP6 proteins (240 pmol). (**C**) EAP20-binding assay by MBP pull-down. One of the GST–CHMP6 fusion proteins (480 pmol) was incubated with amylose resin that carried MBP–EAP20 (approx. 200 pmol). The beads were pelleted by centrifugation, and pulled-down proteins were analysed by SDS/PAGE and visualized by CBB staining. Molecular mass sizes are indicated in kDa.

in the budding yeast. We assumed that CHMP6 might also act as an acceptor for ESCRT-II in mammalian cells using an uncharacterized domain different from the one for interaction with CHMP4. To obtain evidence supporting this hypothesis, we first performed co-immunoprecipitation assays using dissected GFP-fusion protein containing either the N-terminal or C-terminal half of CHMP6. Lysates of HEK-293 cells transfected with the expression vector of FLAG–CHMP4b and that of GFP, CHMP6–GFP, CHMP6NT–GFP or CHMP6CT–GFP were immunoprecipitated with anti-GFP antiserum, and the immunocomplexes were subjected to Western blotting with anti-GFP mAb or anti-FLAG mAb. As shown in Figure 3(A), FLAG–CHMP4b interacted similarly with CHMP6NT–GFP and CHMP6–GFP, but less efficiently with CHMP6CT–GFP. We also examined interactions between CHMP6 and EAP20. As shown in Figure 3(B), FLAG–EAP20 was co-immunoprecipitated with CHMP6–GFP and CHMP6NT–GFP, but not with either CHMP6CT–GFP or the negative control, GFP. Recovery of FLAG–CHMP4b and FLAG–EAP20 in the 10000 ***g*** supernatants (designated 'Input' in Figure 3B) was significantly reduced by co-expression with CHMP6–GFP when compared with the co-expressions with GFP and other GFP-fusion proteins (Figures 3A and 3B), but their expression levels of the FLAG-tagged proteins in the total cell lysates were similar irrespective of the co-expressed GFP fusion proteins (results not shown).

Next, we performed GST pull-down assays to determine whether CHMP4b interacts directly with CHMP6 using purified recombinant proteins. After incubation of various GST-fusion proteins of CHMP6 (GST as a negative control, GST–CHMP6, GST–CHMP6NT and GST–CHMP6CT) with recombinant Trx–His–CHMP4b, glutathione–Sepharose beads were added, and then the proteins bound to the beads were separated by SDS/PAGE and visualized by CBB staining. As shown in Figure 4(A),

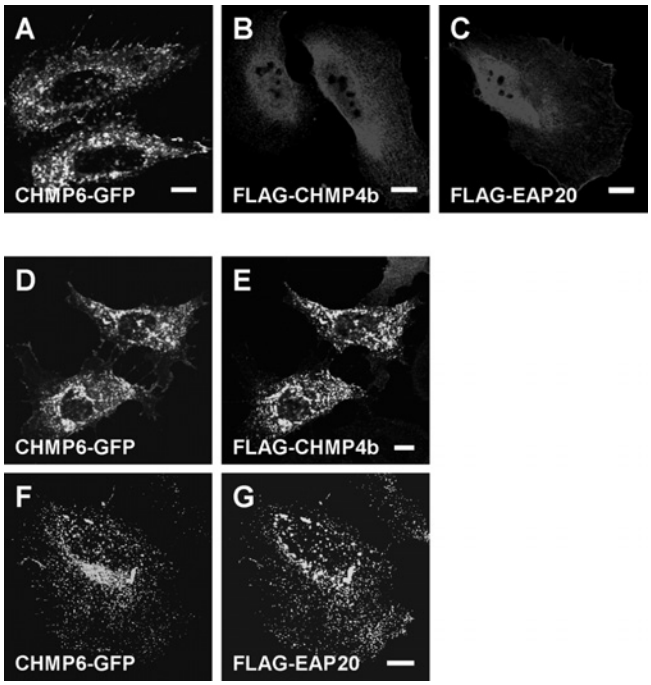

Figure 5 Co-localization of CHMP6–GFP with FLAG–CHMP4b and FLAG–EAP20

HeLa cells transfected independently with pCHMP6-GFP (**A**), pFLAG-CHMP4b (**B**) or pFLAG-EAP20 (**C**), or co-transfected with pCHMP6-GFP and pFLAG-CHMP4b (**D**, **E**) or with pCHMP6-GFP and pFLAG-EAP20 (**F**, **G**) were visualized with a confocal microscope either directly (**A**, **D** and **F**) or by indirect immunofluorescence analyses using anti-FLAG mAb and Cy3-labelled goat anti-mouse IgG (**B**, **C**, **E** and **G**). Scale bars, 10 μm.

Trx–His–CHMP4b was pulled down with GST–CHMP6NT, but, unexpectedly, not with GST–CHMP6. GST–CHMP6CT did not show a positive interaction with Trx–His–CHMP4b compared with GST (a negative control for detection of a background level of the pulled-down protein) under the conditions used. Then direct protein–protein interaction between EAP20 and CHMP6 was analysed using the purified recombinant protein of MBP–EAP20 and the recombinant full-length as well as truncated forms of GST–CHMP6 proteins by pull-down assays. As expected, MBP–EAP20 was pulled-down with GST–CHMP6 and GST–CHMP6NT, but not with either GST–CHMP6CT or GST (Figure 4B). In a reciprocal assay, both GST–CHMP6 and GST–CHMP6NT were pulled down with MBP–EAP20 (Figure 4C) but not with MBP (results not shown). Interaction between MBP–EAP20 and GST–CHMP6CT was not detected either. These results of the *in vitro* CHMP6–EAP20 interaction analyses are consistent with the results obtained from immunoprecipitation assays (Figure 3B).

Punctate subcellular distribution of CHMP6-GFP

We demonstrated previously that transiently overexpressed FLAG–CHMP4b accumulates in a punctate pattern in HEK-293 cells and HeLa cells by confocal microscopic analysis, whereas stably expressed FLAG–CHMP4b exhibits a diffuse pattern, but its accumulation is induced by co-expression with Alix [19]. The rate of accumulation of FLAG–CHMP4b in transient expression experiments depends on its expression level influenced by plasmid amounts and incubation time after transfection (results not shown). In contrast with the punctate subcellular distribution of CHMP6–GFP in 45 % of the transfected cells, as shown in the representative Figure (Figure 5A), the myristoylation-defective mutant CHMP6^{G2A}–GFP was distributed diffusely throughout the cytoplasm and nucleoplasm in 82 % of the transfected cells (see supplementary Figure S2 at http://www.BiochemJ.org/bj/387/bj3870017add.htm). We investigated effects of overexpression of CHMP6–GFP on distributions of FLAG–CHMP4b or FLAG–EAP20 (Figure 5). FLAG–CHMP4b and FLAG–EAP20 were detected throughout the cell diffusely in more than 90 % and 95 % of the transfected cells respectively, as shown in the representative Figures (Figures 5B and 5C), when each protein was expressed independently under the conditions used. On the other hand, FLAG–CHMP4b co-expressed with CHMP6–GFP was distributed in a punctate pattern throughout the cytoplasm, but more in the perinuclear area and almost co-localized with CHMP6–GFP (Figures 5D and 5E). FLAG–EAP20 exhibited a similar punctate and good co-localization with co-expressed CHMP6–GFP (Figures 5F and 5G).

CHMP6–GFP localizes to MVB-related structures

To investigate further the subcellular localization of CHMP6–GFP, we performed organelle marker staining of HeLa cells transfected with pCHMP6-GFP using antibodies against EEA1 (an established marker for early endosomes) and Lamp-1 (a marker of late endosomes and lysosomes) (see supplementary Figure S4 at http://www.BiochemJ.org/bj/387/bj3870017add.htm). Punctate staining of EEA1 was widespread in the cytoplasm of untransfected cells. In contrast, in the cells expressing CHMP6–GFP, some punctate EEA1 staining shifted toward the perinuclear area, where it co-localized partially with CHMP6–GFP. On the other hand, although the distribution of Lamp-1 was not changed dramatically by overexpression of CHMP6–GFP, some co-localization with the accumulating CHMP6–GFP was observed. We stained the cells also with a monoclonal antibody against LBPA, the lipid known to be localized in inner vesicles of MVB (Figures 6A–6C) [2]. LBPA exhibited a punctate distribution throughout the cytoplasm of untransfected cells. Interestingly, in the cells that expressed CHMP6–GFP, the punctate LBPA staining disappeared from the peripheral area, accumulated in the perinuclear area, and merged well with the fluorescent signals of CHMP6–GFP.

CHMP6–GFP overexpression disturbs TfR recycling and cargo sorting of ubiquitinated proteins

We analysed the cellular distribution of TfR to examine effects of CHMP6–GFP overexpression on the TfR-recycling pathway involving the plasma membrane, early endosomes and recycling endosomes. After transfection with pCHMP6-GFP, HeLa cells were fixed, permeabilized with 0.1 % (v/v) Triton-X-100, and stained with anti-TfR mAb using anti-mouse IgG–Cy3 as a secondary antibody (Figures 6D–6F). Fine punctate fluorescent signals of TfR were spread throughout the cytoplasm and along the peripheral area (plasma membrane) of untransfected cells. Conversely, in the cells expressing CHMP6–GFP, fluorescent signals were enhanced in the perinuclear area, where CHMP6–GFP was localized, and the signals in the peripheral area were weaker than those in the untransfected cells. Next, we examined the effect of CHMP6–GFP overexpression on the capacity of TfR to bind Rh–Tf on the cell surface. After transfection, cells were incubated with Rh–Tf for 30 min at 4 °C, washed, fixed, and then subjected to fluorescence microscopy. HeLa cells expressing CHMP6–GFP showed little Rh–Tf binding to their surfaces, indicating the disappearance of most TfR from the plasma membranes (Figures 6G–6I).

Multiple mono-ubiquitination of cell-surface receptors is known to function as a signal for efficient sorting of internalized

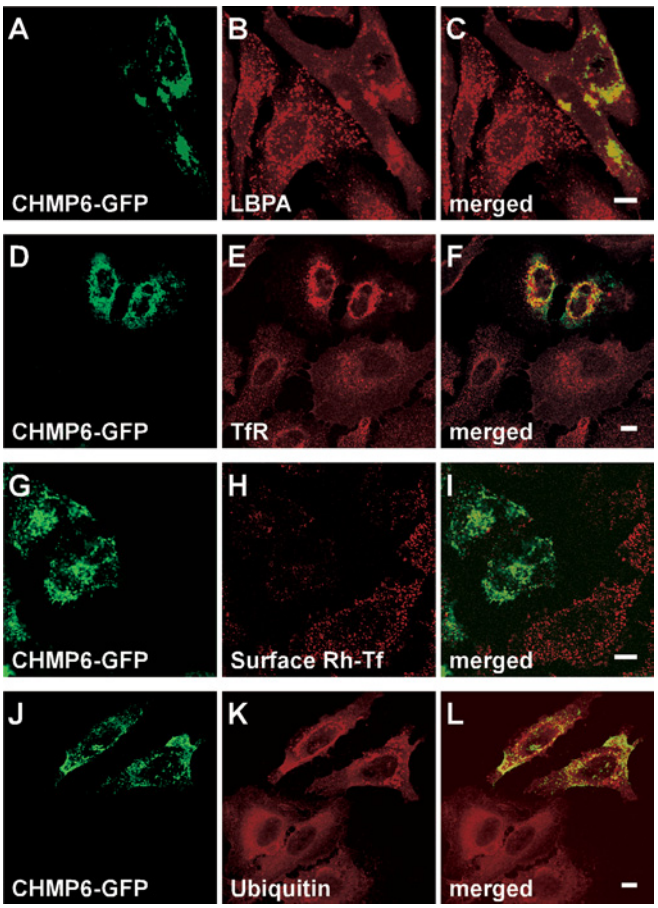

Figure 6 Effects of CHMP6–GFP overexpression on the distribution of LBPA, TfRs and ubiquitinated proteins

(**A**–**F**, **J**–**L**) HeLa cells transfected with pCHMP6-GFP were subjected to immunofluorescence confocal microscopy using monoclonal antibodies against LBPA (**A**–**C**), against TfR (**D**–**F**) and against ubiquitinated proteins (**J**–**L**). (**G**–**I**) HeLa cells transfected with pCHMP6-GFP were incubated at 4 °C for 30 min in the presence of Rh–Tf, washed, and fixed. (**A**, **D**, **G** and **J**) CHMP6–GFP; (**B**) LBPA; (**E**) TfR; (**H**) Rh–Tf binding to TfR on the plasma membrane; (**K**) ubiquitinated proteins; (**C**, **F**, **I** and **L**) merged images. Scale bars, 10 μm.

proteins into luminal vesicles from limited membranes of endosomes during the process of MVB formation [7,23,24]. To determine whether the distribution of ubiquitinated proteins is affected by CHMP6–GFP overexpression, we performed immunostaining of transfected HeLa cells using an anti-ubiquitin mAb (FK2) that recognizes mono- and poly-ubiquitinated proteins, but not free mono-ubiquitin [25]. Compared with CHMP6–GFP-non-expressing cells (Figures 6J–6L, bottom left corner), fluorescent signals of ubiquitinated proteins became stronger and accumulated in a punctate pattern in the perinuclear area of the expressing cells, and partial co-localization of ubiquitinated proteins and CHMP6–GFP was observed (Figures 6J–6L).

Effect of CHMP6–GFP overexpression on the fate of endocytosed EGF

We monitored the fate of endocytosed Rh–EGF, which is first bound to its receptor on the cell surface, then internalized into endosomes, and finally delivered into lysosomes to be degraded. HeLa cells transfected with pCHMP6-GFP were incubated with Rh–EGF at 4 °C for 1 h, washed, and then allowed to uptake Rh–EGF at 37 °C for either 30 min or 5 h. Internalized Rh–EGF observed at 30 min exhibited a punctate distribution similar to that of endosomes. No significant differences were observed between the CHMP6–GFP-expressing and -non-expressing cells, except a slight accumulation of Rh–EGF in the perinuclear area of cells that expressed CHMP6–GFP at a higher level (Figures 7A–7D). At 5 h, however, most of the fluorescent signals of endocytosed Rh–EGF were no longer detectable in the untransfected cells (Figures 7E–7H, asterisks), but they remained in the perinuclear area, where CHMP6–GFP accumulated, in the transfected cells (Figures 7E–7H).

DISCUSSION

ESCRTs are endosomal sorting complexes that are required for transport of ubiquitinated cargo proteins, either derived from the TGN or plasma membrane, into luminal vesicles of the MVB. Yeast genetic and biochemical studies have revealed three ESCRT complexes (ESCRT-I, -II and -III, composed of class E Vps proteins) that are sequentially recruited from the cytosol to endosomal membranes [7]. Although the presence of mammalian orthologues of individual yeast ESCRT components suggests a common MVB sorting system in mammalian cells [26], little is known about the function of ESCRT-III or the mechanism by which this machinery is recruited to the endosomal membrane in the mammalian system. In the present study, we investigated the properties and functions of human CHMP6, which is an orthologue of yeast Vps20 and is expressed ubiquitously in various tissues (see supplementary Figure S1 at http://www.BiochemJ.org/bj/387/bj3870017add.htm).

Although yeast Vps20 was suggested to be N-myristoylated at Gly^2 [9,27], there was no robust evidence of lipid modification of mammalian CHMP6. In the present study, we demonstrated incorporation of [^{3}H]myristate to the WT CHMP6–GFP protein, but not to the Gly^2 mutant $CHMP6^{G2A}$–GFP (Figure 2B, right-hand panel). Exogenously expressed CHMP6–GFP exhibited a punctate distribution throughout the cytoplasm, especially in the perinuclear area, in the transfected HeLa cells by fluorescence microscopic analysis (Figure 5A). On the other hand, the $CHMP6^{G2A}$–GFP mutant exhibited more diffuse distribution (see supplementary Figure S2 at http://www.BiochemJ.org/bj/387/bj3870017add.htm) and could be recovered more in the soluble cytoplasmic fraction than in the organelle fraction by subcellular fractionation (see supplementary Figure S3 at http://www.BiochemJ.org/bj/387/bj3870017add.htm). Recently, a mammalian ESCRT-III component Vps24p (CHMP3/mVps24p) was reported as an effector of PtdIns(3,5)P_2 and PtdIns(3,4)P_2 [28]. According to multiple sequence alignments of mammalian CHMP family members, there is a conserved positively charged amino acid residue (Lys^{49} in mVps24p) in each member. Substitution of aspartate for this lysine residue resulted in a dramatic reduction in the binding ability to liposomes doped with PtdIns(3,5)P_2, which is known to be rich in late endosomes [3]. However, the subcellular localization of the mutant protein $CHMP6^{R49E}$–GFP and that of the WT protein were not significantly different, suggesting that Arg^{49} in CHMP6 is not important for the recruitment of CHMP6 to endosomal membranes.

CHMP6–GFP co-localized well with EEA1 (an early endosomal marker protein) and partially with Lamp-1 (a marker protein for both late endosomes and lysosomes) (see supplementary Figure S4 at http://www.BiochemJ.org/bj/387/bj3870017add.htm) and to a greater extent with LBPA (a marker lipid of late endosomal lumen) (Figures 6A–6C). In contrast with these endosome markers, CHMP6–GFP did not co-localize with an endoplasmic reticulum luminal resident protein, Bip (immunoglobulin heavy-chain-binding protein)/GRP78 (glucose-regulated protein, 78 kDa), or with a cytosolic molecular chaperone protein, Hsp70

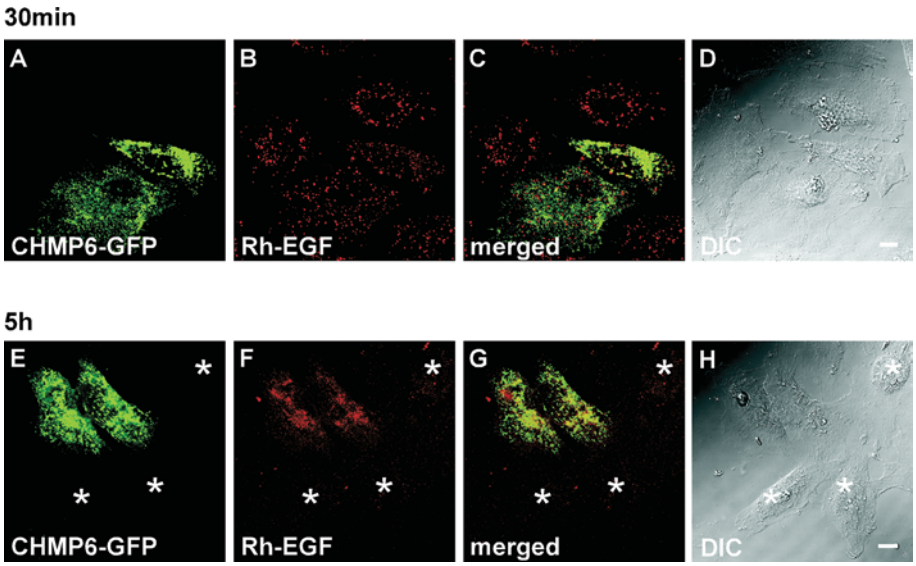

Figure 7 Effects of CHMP6–GFP overexpression on the fate of endocytosed EGF

HeLa cells transfected with pCHMP6-GFP (**A**–**H**) were incubated at 4 °C for 1 h in the presence of Rh–EGF, washed, and then incubated at 37 °C for 30 min (**A**–**D**) or 5 h (**E**–**H**). (**A** and **E**) CHMP6–GFP; (**B** and **F**) Rh–EGF; (**C** and **G**) merged images; (**D** and **H**) differential interference microscopic images. Asterisks indicate untransfected cells. Scale bars, 10 μm.

(heat-shock protein 70) (results not shown). Taken together, the findings suggest that membrane-bound CHMP6–GFP co-localized to endosome-like organelles, including MVBs. These results obtained by fluorescence microscopic analyses are supported further by immunoelectron microscopic data (see supplementary Figure S5 at http://www.BiochemJ.org/bj/387/bj3870017add.htm). Surprisingly, gold particles, indicative of CHMP6–GFP, were detected not only in the limiting, but also in the internal membranes of MVB-like structures. The presence of CHMP6–GFP in the internal membranes of MVB may be related to the dominant-negative effect of the overexpressed CHMP6–GFP on the distribution of LBPA, which is an unconventional acidic lipid specifically present in the MVB, particularly in luminal vesicles [2].

Subcellular distribution of LBPA was significantly affected by overexpression of CHMP6–GFP in HeLa cells (Figures 6A–6C). In contrast with the punctate distribution of LBPA throughout the cytoplasm in untransfected cells, the punctate LBPA staining disappeared from the peripheral area, accumulated in the perinuclear area, and merged well with fluorescent signals of CHMP6–GFP. The ESCRT-III component may influence factors that interact directly or indirectly with LBPA. Matsuo et al. [29] found recently that LBPA by itself can intrinsically induce the formation of MVLs (multivesicular liposomes) *in vitro* under a physiological pH gradient, and that a cytosolic factor, Alix, which is known to bind directly to CHMP4 [14,19,20], is recruited from the cytosol to LBPA-containing liposomes. Although recombinant Alix inhibits MVL formation in an *in vitro* assay, it is essential for MVB formation *in vivo*, and it remains to be established how Alix regulates MVB formation on a molecular basis. Contrary to our expectation that CHMP6 interacts indirectly, if not directly, with Alix *in vivo*, CHMP6–GFP overexpression did not affect the distribution of transiently expressed FLAG–Alix in HeLa cells, and their interaction was not detected by co-immunoprecipitation (results not shown), in agreement with the data presented by von Schwedler et al. [14]. During the course of the present study, it was reported that overexpression of human Vps20/CHMP6 altered cholesterol trafficking and induced the accumulation of cholesterol [30]. This cholesterol accumulation is thought to be due to LBPA accumulation, because LBPA plays an important role in cholesterol trafficking from late endosomes [31]. Thus overexpressed CHMP6–GFP seems to affect the LBPA distribution, not by recruiting Alix, but rather by unknown mechanisms.

Apparent dominant-negative effects of CHMP6–GFP overexpression on the endosomal sorting pathway was also observed for the TfR and endocytosed fluorescence-labelled transferrin (Rh–Tf). While the surface TfR was reduced (Figures 6G–6I), endocytosed TfR accumulated in the perinuclear area, where CHMP6–GFP co-localized (Figures 6D–6F). These findings suggest inhibition of TfR recycling and/or inhibition of newly synthesized TfR transport to the cell surface via endosomes [32]. Moreover, the delivery system from endosomes to lysosomes through the MVB pathway appears to be impaired by CHMP6–GFP overexpression, as demonstrated by accumulation of ubiquitinated proteins (Figures 6J–6L) and endocytosed Rh–EGF (Figure 7, lower panels) in the perinuclear area, whereas a dominant-negative effect is not exerted in earlier processes of endocytosis that involve uptake of Rh–EGF at the plasma membrane and subsequent transport to early endosomal compartments (Figure 7, upper panels). These observed dominant-negative effects of CHMP6–GFP on the endosomal pathway are similar to those of $SKD1^{E235Q}$ (suppressor of potassium transport growth defect 1 with a $Glu^{235} \rightarrow Gln$ mutation), a dominant-negative mutant of AAA-type ATPase SKD1/Vps4B [19,22]. Overexpression of GFP–$SKD1^{E235Q}$ causes formation of aberrant endosomes, the so-called E235Q compartment, by a blockade of membrane efflux from sorting endosomes, where membrane influx into the compartment is normal. CHMP6–GFP co-localized with Myc–$SKD1^{E235Q}$ in the co-transfected HeLa cells (results not shown), probably by physical association, either directly or indirectly, as suggested by the results of yeast two-hybrid assays for all combinations of human class E Vps proteins [14,15]. CHMP6–GFP overexpression may cause sequestration of Vps4 and/or EAP20, and may accumulate indirectly other ESCRT proteins, as well as LBPA, on endosomes simply by gumming up the endosomal system, and impair normal sorting of the endocytosed receptors.

Although the two recent reports of yeast two-hybrid assays suggest positive interactions between CHMP4 isoforms and CHMP6 [14,15], Peck et al. [30] failed to demonstrate the interactions by the GST pull-down assays using GST–hSnf7-1/CHMP4b and lysates of Cos1 cells overexpressing hVps20/CHMP6. In the present study, we demonstrated the interactions between CHMP6 and CHMP4b as well as between CHMP6 and EAP20 by co-immunoprecipitation (Figure 3), GST or MBP pull-down assays using recombinant proteins (Figure 4) and by subcellular co-localization in the transfected HeLa cells (Figure 5). It was suggested that CHMP4b interacts with CHMP6 through the N-terminal region of CHMP6 (Figures 3A and 4A). The interaction between FLAG–CHMP4b and the N-myristoylation-defective mutant CHMP6^{G2A}–GFP was not efficient compared with that in the case of CHMP6–GFP (results not shown). GST pull-down assays using recombinant proteins showed that Trx–His–CHMP4b interacted with the N-terminal half CHMP6 (GST–CHMP6NT) directly *in vitro*, but not with full-length CHMP6 (GST–CHMP6) or C-terminal half CHMP6 (GST–CHMP6CT) (Figure 4A). These results suggest that the requirement of CHMP6 for the interaction with CHMP4b is not N-myristoylation of the former protein, but rather accessibility of the CHMP6 N-terminal region, which is influenced by a molecule tagged at the N-terminus, i.e. a large protein (GST) or myristate plus membrane. Indeed, interaction between GFP–CHMP6 (an N-terminally GFP-tagged protein lacking a myristoylation site) and FLAG–CHMP4b was as strong as that between CHMP6–GFP and FLAG–CHMP4b in the co-immunoprecipitation assay (results not shown). The apparent negative interaction between full-length CHMP6 and full-length CHMP4b in the *in vitro* pull-down assay using recombinant proteins (Figure 4A), but positive interaction *in vivo* (Figure 3A), may be explained as follows: CHMP family members involving CHMP6 and CHMP4b are highly charged with unevenly distributed basic and acid residues in the N- and C-terminal halves respectively, and they may therefore fold in half with a closed conformation or they may form homodimers. Upon transient binding to the membrane with N-terminal myristoyl moiety, CHMP6 may change its conformation to open its N-terminal region for CHMP4 binding in a way similar to that proposed for a myristoyl switch protein [33]. Another possible explanation is the presence of a factor(s) that induces conformational change in CHMP6. Such a candidate is EAP20, a member of ESCRT-II, because the full-length EAP20 protein fused with MBP interacted with GST–CHMP6 as efficiently as it did with GST–CHMP6NT *in vitro*, but did not interact with GST–CHMP6CT in either GST pull-down (Figure 4B) or MBP pull-down assays (Figure 4C). Alix, known as a protein that interacts with a penta-EF-hand calcium-binding protein, ALG-2 [34–36], may also be a candidate for the induction of conformational change in, in this case, CHMP4b. A head-to-tail complex formation based on electrostatic interactions, as well as coiled-coil-dependent binding (N-terminal half, basic; C-terminal half, acidic), might explain detection of interaction between CHMP6CT–GFP and FLAG–CHMP4b *in vivo* (Figure 3A), but not *in vitro*, using recombinant proteins (Figure 4A). While the present paper was being revised, the crystal structure of yeast ESCRT-II complex was reported by two independent groups [37,38]. The trilobal or Y-shaped complex contains two copies of Vps25 and a copy of Vps22 and Vps36. Regardless of absence of apparent similarity in primary structure, each ESCRT-II component possesses tandem repeats of a common building block called WH (winged helix). Moreover, Teo et al. [38] reported that yeast Vps25 interacts directly with non-myristoylated recombinant Vps20, and increases liposome binding of the complex *in vitro*. Further studies are required to investigate whether human CHMP6 interacts directly with other ESCRT-II components (EAP30 and EAP45) and to identify potential membrane binding site(s) in the complexes of ESCRT-II and -III, other than the myristoyl moiety of CHMP6.

The assembly system of ESCRT-III in mammalian cells may be far more complicated than the originally proposed yeast system because of the presence of additional homologous ESCRT-III components: CHMP1 and CHMP5, two isoforms in CHMP2 and three isoforms in CHMP4. Recent high-throughput protein–protein interaction analyses of class E Vps proteins of yeast [39] and of human orthologues [14,15] have revealed some differences between ESCRT-III-associating proteins in humans and yeast. In humans, Alix bridges ESCRT-I and ESCRT-III by interacting with a component of the respective ESCRT, i.e. Tsg101 and CHMP4 respectively. Yeast has two Alix homologues named Bro1 and Rim20. Both of them interact with Vps32/Snf7 (an orthologue of CHMP4), but they do not interact with the Vps23 (an orthologue of Tsg101). Instead, Vps20 associates with Vps28 as well as with Vps37, components of ESCRT-I. Thus recruiting of ESCRT-III to endosomal membranes in mammalian cells may have adopted a different regulatory system still undefined from yeast genetic studies on class E Vps proteins. Interestingly, Bro1 was recently suggested to act at a late step of MVB sorting, probably after the ESCRT-III core components and before or in conjunction with the Doa4-deubiquitinating enzyme in the yeast [40]. Further studies to identify new ESCRT-associating proteins should lead to clarification of the regulatory mechanism of MVB sorting.

We thank Dr T. Yoshimori for providing a monoclonal antibody against TfR and for his valuable discussions, and we thank F. Kaji for his photographic work. We are grateful to Dr K. Hitomi for his encouraging suggestions. This work was supported by a Grant-in-Aid for Scientific Research B (to M. M.) and a Grant-in-Aid for Young Scientist B (to H. S.).

REFERENCES

1 Maxfield, F. R. and McGraw, T. E. (2004) Endocytic recycling. Nat. Rev. Mol. Cell Biol. **5**, 121–132
2 Kobayashi, T., Stang, E., Fang, K. S., de Moerloose, P., Parton, R. G. and Gruenberg, J. (1998) A lipid associated with the antiphospholipid syndrome regulates endosome structure and function. Nature (London) **392**, 193–197
3 Mukherjee, S. and Maxfield, F. R. (2000) Role of membrane organization and membrane domains in endocytic lipid trafficking. Traffic **1**, 203–211
4 Gruenberg, J. and Stenmark, H. (2004) The biogenesis of multivesicular endosomes. Nat. Rev. Mol. Cell Biol. **5**, 317–323
5 Di Fiore, P. P., Polo, S. and Hofmann, K. (2003) When ubiquitin meets ubiquitin receptors: a signalling connection. Nat. Rev. Mol. Cell Biol. **4**, 491–497
6 Haglund, K., Di Fiore, P. P. and Dikic, I. (2003) Distinct monoubiquitin signals in receptor endocytosis. Trends Biochem. Sci. **28**, 598–603
7 Katzmann, D. J., Odorizzi, G. and Emr, S. D. (2002) Receptor downregulation and multivesicular-body sorting. Nat. Rev. Mol. Cell Biol. **3**, 893–905
8 Katzmann, D. J., Babst, M. and Emr, S. D. (2001) Ubiquitin-dependent sorting into the multivesicular body pathway requires the function of a conserved endosomal protein sorting complex, ESCRT-I. Cell **106**, 145–155
9 Babst, M., Katzmann, D. J., Estepa-Sabal, E. J., Meerloo, T. and Emr, S. D. (2002) ESCRT-III: an endosome-associated heterooligomeric protein complex required for MVB sorting. Dev. Cell **3**, 271–282
10 Babst, M., Katzmann, D. J., Snyder, W. B., Wendland, B. and Emr, S. D. (2002) Endosome-associated complex, ESCRT-II, recruits transport machinery for protein sorting at the multivesicular body. Dev. Cell **3**, 283–289
11 Katzmann, D. J., Stefan, C. J., Babst, M. and Emr, S. D. (2003) Vps27 recruits ESCRT machinery to endosomes during MVB sorting. J. Cell Biol. **162**, 413–423
12 Bilodeau, P. S., Winistorfer, S. C., Kearney, W. R., Robertson, A. D. and Piper, R. C. (2003) Vps27-Hse1 and ESCRT-I complexes cooperate to increase efficiency of sorting ubiquitinated proteins at the endosome. J. Cell Biol. **163**, 237–243
13 Strack, B., Calistri, A., Craig, S., Popova, E. and Gottlinger, H. G. (2003) AIP1/ALIX is a binding partner for HIV-1 p6 and EIAV p9 functioning in virus budding. Cell **114**, 689–699
14 von Schwedler, U. K., Stuchell, M., Muller, B., Ward, D. M., Chung, H. Y., Morita, E., Wang, H. E., Davis, T., He, G. P., Cimbora, D. M. et al. (2003) The protein network of HIV budding. Cell **114**, 701–713

15 Martin-Serrano, J., Yarovoy, A., Perez-Caballero, D. and Bieniasz, P. D. (2003) Divergent retroviral late-budding domains recruit vacuolar protein sorting factors by using alternative adaptor proteins. Proc. Natl. Acad. Sci. U.S.A. **100**, 12414–12419
16 Pornillos, O., Garrus, J. E. and Sundquist, W. I. (2002) Mechanisms of enveloped RNA virus budding. Trends Cell Biol. **12**, 569–579
17 Clague, M. J. and Urbé, S. (2003) Hrs function: viruses provide the clue. Trends Cell Biol. **13**, 603–606
18 Howard, T. L., Stauffer, D. R., Degnin, C. R. and Hollenberg, S. M. (2001) CHMP1 functions as a member of a newly defined family of vesicle trafficking proteins. J. Cell Sci. **114**, 2395–2404
19 Katoh, K., Shibata, H., Suzuki, H., Nara, A., Ishidoh, K., Kominami, E., Yoshimori, T. and Maki, M. (2003) The ALG-2-interacting protein Alix associates with CHMP4b, a human homologue of yeast Snf7 that is involved in multivesicular body sorting. J. Biol. Chem. **278**, 39104–39113
20 Katoh, K., Shibata, H., Hatta, K. and Maki, M. (2004) CHMP4b is a major binding partner of the ALG-2-interacting protein Alix among the three CHMP4 isoforms. Arch. Biochem. Biophys. **421**, 159–165
21 Shibata, H., Yamada, K., Mizuno, T., Yorikawa, C., Takahashi, H., Satoh, H., Kitaura, Y. and Maki, M. (2004) The penta-EF-hand protein ALG-2 interacts with a region containing PxY repeats in Alix/AIP1, which is required for the subcellular punctate distribution of the amino-terminal truncation form of Alix/AIP1. J. Biochem. **135**, 117–128
22 Yoshimori, T., Yamagata, F., Yamamoto, A., Mizushima, N., Kabeya, Y., Nara, A., Miwako, I., Ohashi, M., Ohsumi, M. and Ohsumi, Y. (2000) The mouse SKD1, a homologue of yeast Vps4p, is required for normal endosomal trafficking and morphology in mammalian cells. Mol. Biol. Cell **11**, 747–763
23 Pelham, H. R. (2002) Insights from yeast endosomes. Curr. Opin. Cell Biol. **14**, 454–462
24 Sorkin, A. and von Zastrow, M. (2002) Signal transduction and endocytosis: close encounters of many kinds. Nat. Rev. Mol. Cell Biol. **3**, 600–614
25 Haglund, K., Sigismund, S., Polo, S., Szymkiewicz, I., Di Fiore, P. P. and Dikic, I. (2003) Multiple monoubiquitination of RTKs is sufficient for their endocytosis and degradation. Nat. Cell Biol. **5**, 461–466
26 Raiborg, C., Rusten, T. E. and Stenmark, H. (2003) Protein sorting into multivesicular endosomes. Curr. Opin. Cell Biol. **15**, 446–455
27 Ashrafi, K., Farazi, T. A. and Gordon, J. I. (1998) A role for *Saccharomyces cerevisiae* fatty acid activation protein 4 in regulating protein N-myristoylation during entry into stationary phase. J. Biol. Chem. **273**, 25864–25874
28 Whitley, P., Reaves, B. J., Hashimoto, M., Riley, A. M., Potter, B. V. and Holman, G. D. (2003) Identification of mammalian Vps24p as an effector of phosphatidylinositol 3,5-bisphosphate-dependent endosome compartmentalization. J. Biol. Chem. **278**, 38786–38795
29 Matsuo, H., Chevallier, J., Mayran, N., Le Blanc, I., Ferguson, C., Faure, J., Blanc, N. S., Matile, S., Dubochet, J., Sadoul, R. et al. (2004) Role of LBPA and Alix in multivesicular liposome formation and endosome organization. Science **303**, 531–534
30 Peck, J. W., Bowden, E. T. and Burbelo, P. D. (2004) Structure and function of human Vps20 and Snf7 proteins. Biochem. J. **377**, 693–700
31 Kobayashi, T., Beuchat, M. H., Lindsay, M., Frias, S., Palmiter, R. D., Sakuraba, H., Parton, R. G. and Gruenberg, J. (1999) Late endosomal membranes rich in lysobisphosphatidic acid regulate cholesterol transport. Nat. Cell Biol. **1**, 113–118
32 Futter, C. E., Connolly, C. N., Cutler, D. F. and Hopkins, C. R. (1995) Newly synthesized transferrin receptors can be detected in the endosome before they appear on the cell surface. J. Biol. Chem. **270**, 10999–11003
33 Ames, J. B., Tanaka, T., Stryer, L. and Ikura, M. (1996) Portrait of a myristoyl switch protein. Curr. Opin. Struct. Biol. **6**, 432–438
34 Missotten, M., Nichols, A., Rieger, K. and Sadoul, R. (1999) Alix, a novel mouse protein undergoing calcium-dependent interaction with the apoptosis-linked-gene 2 (ALG-2) protein. Cell Death Differ. **6**, 124–129
35 Vito, P., Pellegrini, L., Guiet, C. and D'Adamio, L. (1999) Cloning of AIP1, a novel protein that associates with the apoptosis-linked gene ALG-2 in a Ca^{2+}-dependent reaction. J. Biol. Chem. **274**, 1533–1540
36 Maki, M., Kitaura, Y., Satoh, H., Ohkouchi, S. and Shibata, H. (2002) Structures, functions and molecular evolution of the penta-EF-hand Ca^{2+}-binding proteins. Biochim. Biophys. Acta **1600**, 51–60
37 Hierro, A., Sun, J., Rusnak, A. S., Kim, J., Prag, G., Emr, S. D. and Hurley, J. H. (2004) Structure of the ESCRT-II endosomal trafficking complex. Nature (London) **431**, 221–225
38 Teo, H., Perisic, O., González, B. and Williams, R. L. (2004) ESCRT-II, an endosome-associated complex required for protein sorting: crystal structure and interactions with ESCRT-III and membranes. Dev. Cell **7**, 559–569
39 Bowers, K., Lottridge, J., Helliwell, S. B., Goldthwaite, L. M., Luzio, J. P. and Stevens, T. H. (2004) Protein–protein interactions of ESCRT complexes in the yeast *Saccharomyces cerevisiae*. Traffic **5**, 194–210
40 Nikko, E., Marini, A. M. and André, B. (2003) Permease recycling and ubiquitination status reveal a particular role for Bro1 in the multivesicular body pathway. J. Biol. Chem. **278**, 50732–50743

Received 20 July 2004/13 October 2004; accepted 28 October 2004
Published as BJ Immediate Publication 28 October 2004, DOI 10.1042/BJ20041227